Defect Detection Using Hidden Markov Random Fields

Aleksandar Dogandži, Nawanat Euaanant, and Benhong Zhang

Citation: AIP Conference Proceedings **760**, 704 (2005); doi: 10.1063/1.1916744
View online: http://dx.doi.org/10.1063/1.1916744
View Table of Contents:
http://scitation.aip.org/content/aip/proceeding/aipcp/760?ver=pdfcov
Published by the AIP Publishing

DEFECT DETECTION USING HIDDEN MARKOV RANDOM FIELDS

Aleksandar Dogandžić, Nawanat Eua-anant, and Benhong Zhang

Iowa State University, Center for Nondestructive Evaluation,
1915 Scholl Road, Ames, IA 50011, USA

ABSTRACT. We derive an approximate maximum *a posteriori* (MAP) method for detecting NDE defect signals using hidden Markov random fields (HMRFs). In the proposed HMRF framework, a set of spatially distributed NDE measurements is assumed to form a noisy realization of an underlying random field that has a simple structure with Markovian dependence. Here, the random field describes the defect signals to be estimated or detected. The HMRF models incorporate measurement locations into the statistical analysis, which is important in scenarios where the same defect affects measurements at multiple locations. We also discuss initialization of the proposed HMRF detector and apply to simulated eddy-current data and experimental ultrasonic C-scan data from an inspection of a cylindrical Ti 6-4 billet.

INTRODUCTION

In nondestructive evaluation (NDE) applications, defect signal typically affects multiple measurements at neighboring spatial locations. Therefore, multiple spatial measurements should be incorporated into defect detection algorithms, leading to an improved performance compared with the detectors that ignore spatial dependence. Markov random field models have been widely used to describe spatially distributed random phenomena, see e.g. [1]–[3]. In this paper, we propose a hidden Markov random field (HMRF) model to describe spatially distributed NDE observations. Under this model, the observations form a noisy realization of an underlying random field that has a simple structure with Markovian dependence. Here, the Markovian assumption implies that the random field at a particular measurement location is modeled in terms of field values at neighboring spatial locations. We show how the proposed HMRF model can be used to efficiently remove false alarms and detect potential defect regions.

We first introduce the proposed HMRF models and present an approximate maximum *a posteriori* (MAP) algorithm for defect detection. We then apply the proposed methods to simulated and experimental NDE data. Finally, we conclude by outlining suggestions for future work.

CP760, *Review of Quantitative Nondestructive Evaluation Vol. 24,* ed. by D. O. Thompson and D. E. Chimenti

HMRF MODEL

Assume that we have collected K spatially distributed measurements $y_k, k = 1, \ldots, K$, modeled as an HMRF:

- $y_k,\ k = 1, 2, \ldots, K$ are conditionally independent random variables with probability distributions $p_{y_k|\beta_k}(y_k|\beta_k; \boldsymbol{\upsilon})$ describing the *measurement-error (noise) model* and
- $\beta_k,\ k = 1, 2, \ldots, K$ form a *Markov random field* (MRF) describing a *process model*.

In this paper, we focus on the Gaussian measurement-error model:

$$p_{y_k|\beta_k}(y_k|\beta_k; \boldsymbol{\upsilon}) = g\Big(y_k;\ \mu(\beta_k), \sigma^2(\beta_k)\Big) = \frac{1}{\sqrt{2\pi\sigma^2(\beta_k)}} \cdot \exp\Big\{ -\frac{[y_k - \mu(\beta_k)]^2}{2\,\sigma^2(\beta_k)} \Big\} \quad (1)$$

where $\boldsymbol{\upsilon} = [\mu(0), \sigma^2(0), \mu(1), \sigma^2(1)]^T$ is the vector of measurement-error model parameters. Here, "^{T}" denotes a transpose and $g(y;\ \mu, \sigma^2)$ the Gaussian probability density function (pdf) having mean μ and variance σ^2. The process model is described by the Ising MRF with the kth location corresponding one of the following two classes:

- "defect present" ($\beta_k = 1$) and
- "defect absent" ($\beta_k = 0$).

Under the Ising model, the probability mass function (pmf) of β_k is given by (see e.g. [1, ch. 6.5])

$$P[\beta_k = 1 \mid \mathcal{N}(k)] = \frac{\exp(\delta\, u_k)}{1 + \exp(\delta\, u_k)} \quad (2)$$

where $\mathcal{N}(k)$ denotes the neighborhood of the kth measurement location, δ is a non-negative constant (tuning parameter) describing the field strength, and

$$u_k = \sum_{l \in \mathcal{N}(k)} (2\beta_l - 1)$$

is the difference between the numbers of neighbors of the measurement location k that belong to classes 1 and 0, respectively. Hence, u_k is positive if class 1 prevails in the neighborhood $\mathcal{N}(k)$, negative if class 0 prevails, and zero if the neighbors are equally distributed between the two classes.

Our goal is to detect defect signals or, equivalently, estimate the MRF $\boldsymbol{\beta} = [\beta_1, \beta_2, \ldots, \beta_K]^T$. We first describe an approximate MAP algorithm for defect detection assuming that the measurement-error model parameters $\boldsymbol{\upsilon}$ are known. We then develop an alternating-projection algorithm for jointly estimating $\boldsymbol{\beta}$ and $\boldsymbol{\upsilon}$ in the case where the measurement-error model parameters are unknown and discuss the initialization of the proposed iteration.

APPROXIMATE MAP DETECTION

We utilize the *iterated conditional modes* (ICM) algorithm in [2] to obtain approximate MAP estimates of the MRF $\boldsymbol{\beta}$. Under the Ising MRF model (2), the ICM algorithm updates β_k at the kth measurement location by maximizing the "local" (conditional) MAP objective function:

$$\widehat{\beta}_k = \begin{cases} 1, & \ln\big[p_{y_k|\beta_k}(y_k \,|\, 1;\, \boldsymbol{\upsilon}) \big/ p_{y_k|\beta_k}(y_k \,|\, 0;\, \boldsymbol{\upsilon})\big] + \delta\, u_k > 0 \\ 0, & \text{otherwise} \end{cases} . \quad (3a)$$

When applied to each k in turn, this procedure defines a single cycle of the ICM algorithm. The cycling is performed until convergence, i.e. until the estimates of β_k do not change significantly for all $k \in \{1, 2, \ldots, K\}$. Under the Gaussian measurement-error model in (1), the approximate MAP decision rule (3a) further simplifies: select $\widehat{\beta}_k = 1$ if

$$-\tfrac{1}{2}\ln\sigma^2(1) - \frac{[y_k - \mu(1)]^2}{2\sigma^2(1)} + \tfrac{1}{2}\ln\sigma^2(0) + \frac{[y_k - \mu(0)]^2}{2\sigma^2(0)} + \delta u_k > 0 \tag{3b}$$

otherwise, select $\widehat{\beta}_k = 0$. The above approximate MAP detector is based on the assumption that the measurement-error model parameters $\boldsymbol{\upsilon}$ are *known*. We now propose an alternating-projection algorithm that jointly estimates $\boldsymbol{\upsilon}$ and the MRF $\boldsymbol{\beta}$ by iterating between the following two steps:

(i) Approximate MAP Detection: Fix the measurement-error model parameters $\boldsymbol{\upsilon} = \widehat{\boldsymbol{\upsilon}}$ and update the MRF $\boldsymbol{\beta}$ using *one cycle* of the approximate MAP algorithm;

(ii) Measurement-Error Model Parameter Estimation: Fix $\boldsymbol{\beta}$ and estimate $\boldsymbol{\upsilon}$ by maximizing the log-likelihood function for known $\boldsymbol{\beta}$, $\sum_{k=1}^{K} \ln\big[p_{y_k|\beta_k}(\boldsymbol{y}_k \,|\, \beta_k;\, \boldsymbol{\upsilon})\big]$, yielding the following sample means and variances:

$$\widehat{\mu}(1) \;=\; \frac{1}{K_1}\sum_{k=1}^{K}\beta_k\, y_k, \quad \widehat{\mu}(0) = \frac{1}{K - K_1}\sum_{k=1}^{K}(1-\beta_k)\, y_k \tag{4a}$$

$$\widehat{\sigma}^2(1) \;=\; \frac{1}{K_1}\Big[\sum_{k=1}^{K}\beta_k\, y_k^2\Big] - \widehat{\mu}^2(1), \;\; \widehat{\sigma}^2(0) = \frac{1}{K - K_1}\Big[\sum_{k=1}^{K}(1-\beta_k)\, y_k^2\Big] - \widehat{\mu}^2(0) \tag{4b}$$

where $K_1 = \sum_{k=1}^{K}\beta_k$ is the number of measurement locations with defect signals [according to the detection results from Step (i)].

Choosing the Initial Estimates of the Measurement-error Model Parameters

To implement the above iteration successfully, we need a good initial estimate $\boldsymbol{\upsilon}_{\text{init}} = [\mu_{\text{init}}(0), \sigma^2_{\text{init}}(0), \mu_{\text{init}}(1), \sigma^2_{\text{init}}(1)]^T$ of the model-parameter vector. Here, we compute $\boldsymbol{\upsilon}_{\text{init}}$ using the ML clustering algorithm which ignores the spatial dependence. We also estimate the prior probability $\pi(1)$ that a measurement location belongs to a defect region. The ML clustering algorithm consists of the following iterations:

(i) Choose initial estimates $\boldsymbol{\upsilon}^{(0)}_{\text{init}}$ and $\pi^{(0)}(1)$, and compute $\pi^{(0)}(0) = 1 - \pi^{(0)}(1)$.

(ii) Having calculated $\pi^{(i)}(1), \pi^{(i)}(0)$, and $\boldsymbol{\upsilon}^{(i)}_{\text{init}}$, compute new estimates

$$\pi^{(i+1)}(\xi) \;=\; \frac{1}{K}\sum_{k=1}^{K} q_k^{(i)}(\xi) \tag{5a}$$

$$\mu^{(i+1)}_{\text{init}}(\xi) \;=\; \frac{1}{K\,\pi^{(i+1)}(\xi)}\sum_{k=1}^{K} q_k^{(i)}(\xi)\, y_k \tag{5b}$$

$$\big[\sigma^2_{\text{init}}(\xi)\big]^{(i+1)} \;=\; \frac{1}{K\,\pi^{(i+1)}(\xi)}\sum_{k=1}^{K} q_k^{(i)}(\xi)\,[y_k - \mu^{(i+1)}(\xi)]^2 \tag{5c}$$

$$q_k^{(i+1)}(\xi) \;=\; \frac{\pi^{(i+1)}(\xi)\cdot g\big(y_k; \mu^{(i+1)}(\xi), [\sigma^2(\xi)]^{(i+1)}\big)}{\sum_{d=0}^{1}\pi^{(i+1)}(d)\cdot g\big(y_k; \mu^{(i+1)}(d), [\sigma^2(d)]^{(i+1)}\big)} \tag{5d}$$

for $\xi \in \{0, 1\}$ and $k = 1, 2, \ldots, K$.

(iii) When $\mu_{\text{init}}^{(i+1)}(\xi) = \mu_{\text{init}}^{(i)}(\xi)$ and $[\sigma_{\text{init}}^2(\xi)]^{(i+1)} = [\sigma_{\text{init}}^2(\xi)]^{(i)}$ for $\xi \in \{0, 1\}$ then stop. Otherwise increase the iteration number i by 1 and go to step (ii).

Apart from having a different exit criterion [i.e. step (iii)], the above algorithm is identical to the ML clustering algorithm in e.g. [4, pp. 529–530] and [5, ch. 3.3.1]. In the following, we present numerical examples.

EXAMPLES

Simulated Eddy-current Data

Figure 1(a) shows a magnitude plot of low-noise experimental eddy-current impedance measurements in a sample containing two realistic flaws, where each pixel corresponds to a measurement location. To simulate noisy measurements, we added independent, identically distributed (i.i.d.) zero-mean complex Gaussian noise yielding the magnitude plot in Figure 1(b). We first apply an energy detector to the noisy data and then utilize the proposed approximate MAP method to remove false alarms. A testing window $\boldsymbol{Y}_{\text{T}}$ of size 10×10 was swept across the noisy image. At each window location, we computed the energy-detector test statistic:

$$\begin{aligned} \text{ED} &= (2/\sigma^2) \cdot \text{tr}(\boldsymbol{Y}_{\text{T}} \boldsymbol{Y}_{\text{T}}^H) \\ &= (2/\sigma^2) \cdot (\text{sum of squared magnitudes of all pixels in } \boldsymbol{Y}_{\text{T}}) \end{aligned}$$

where, in this example, the noise variance was $\sigma^2 = 0.4$. In the absence of defect signal, the ED test statistic is distributed as a χ^2 random variable with $2md$ degrees of freedom. Figure 2(a) shows the (logarithms of) ED test statistics. In Figure 2(b), black pixels correspond to the test values [from Figure 2(a)] that were larger than a a specified threshold. The threshold was set to guarantee the false-alarm probability $P_{\text{FA}} = 1\%$. We now apply the approximate MAP algorithm to the ED results in Figure 2(a) using a 5×5 neighborhood shown in Figure 3. [Here, the MAP algorithm is initialized by the results of the ML clustering algorithm and the ML clustering algorithm is initialized using the energy-detector results in Figure 2(b).] In Figure 4, we show the results of the MAP algorithm for the field strength $\delta = 2$. Clearly, the MAP detector removes the false alarms caused by the energy detector.

Experimental Ultrasonic Data

We now apply the approximate MAP method to experimental ultrasonic C-scan data from an inspection of a cylindrical Ti 6-4 billet. The sample, taken from the contaminated billet, contains 17 # 2 flat bottom holes at 3.2" depth. The ultrasonic data were collected in a single experiment by moving a probe along the axial direction and scanning the billet along the circumferential direction at each axial position. The raw C-scan data with marked defects are shown in Figure 5. The vertical coordinate is proportional to rotation angle and the horizontal coordinate to axial position. We consider two approaches to construct the HMRF observations y_k:

- subtracting row means from the C-scan image and
- using generalized likelihood ratio (GLR) test statistics for correlated noise in [6].

Using the first approach with a 7×3 neighborhood (shown in Figure 6) and the field strength $\delta = 2.5$, the MAP detector yields the results in Figure 7. All defects are successfully detected

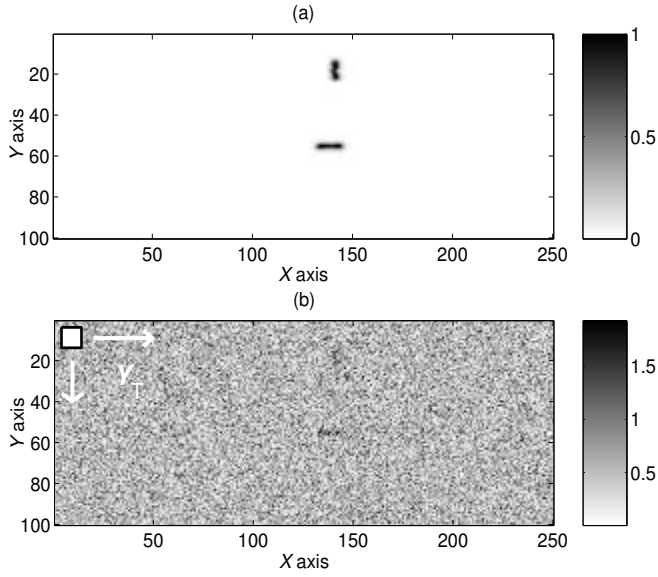

FIGURE 1. (a) Magnitude plot of low-noise eddy-current measurements with peak value normalized to one and (b) magnitude plot of eddy-current data in (a) corrupted by complex white Gaussian noise with variance $\sigma^2 = 0.4$.

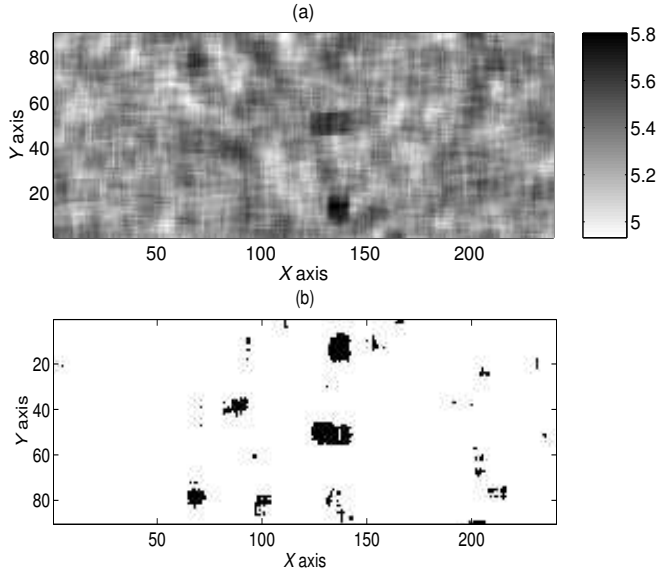

FIGURE 2. (a) Logarithms of ED test statistics and (b) energy-detector results for $P_{\mathrm{FA}} = 1\%$.

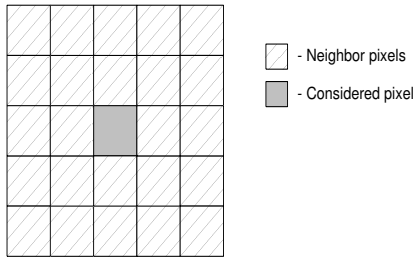

FIGURE 3. A 5×5 neighborhood used to remove false alarms from the ED results in Figure 2.

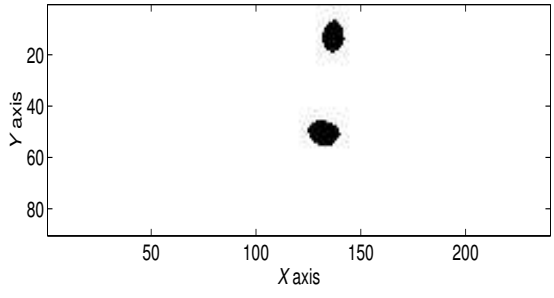

FIGURE 4. Results of the MAP detector applied to the ED image in Figure 2, for $\delta = 2$.

and there is one false-alarm region. We now apply the second approach where the GLR test statistics are computed using a testing window of size 5×5 around the measurement location of interest. The GLR test statistics and detection results for $P_{\rm FA} = 1\%$ are shown in Figure 8. Since the GLR test yields enlarged defect areas, we use a larger neighborhood with a 7×5 window (see Figure 9) and a larger field strength $\delta = 3.5$. Applying the MAP algorithm to the GLR test results yields the best performance with no false alarms, see Figure 10.

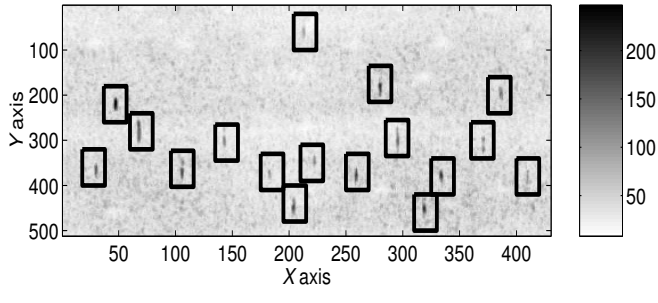

FIGURE 5. Ultrasonic C-scan data with 17 defects.

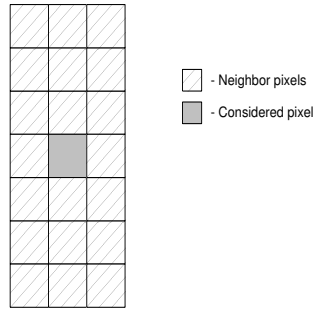

FIGURE 6. A 7×3 neighborhood used to analyze the ultrasonic C-scan image in Figure 5.

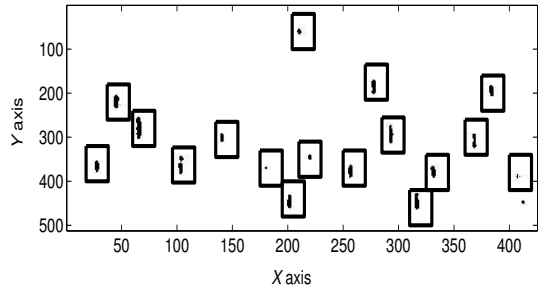

FIGURE 7. Results of the MAP detector applied to the ultrasonic C-scan data, for $\delta = 2.5$.

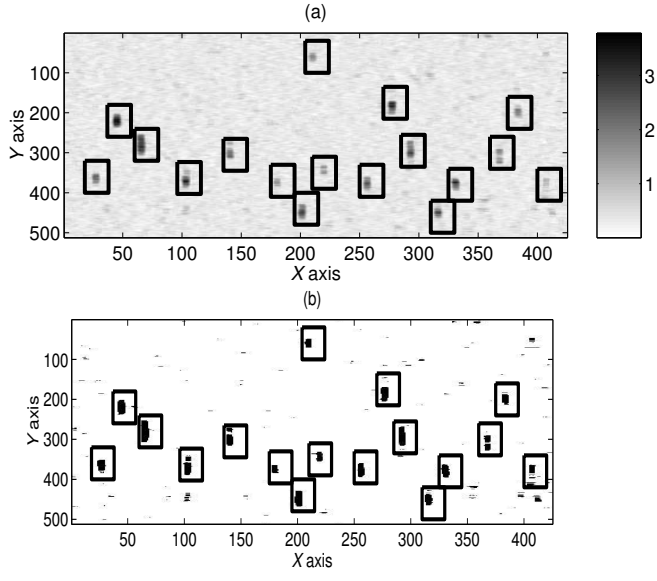

FIGURE 8. (a) GLR test statistics and (b) GLR detector results for $P_{\mathrm{FA}} = 1\%$.

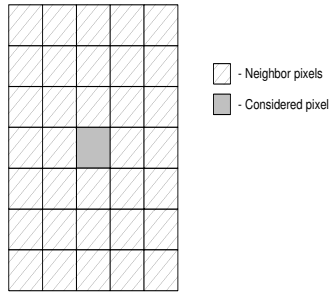

FIGURE 9. 7×5 neighborhood used to remove false alarms from the GLR results in Figure 8.

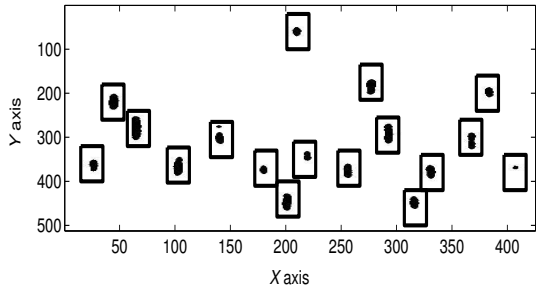

FIGURE 10. Results of the MAP detector applied to the GLR image in Figure 8, for $\delta = 3.5$.

CONCLUSIONS

We developed an approximate maximum *a posteriori* defect detector for hidden Markov random fields with Gaussian measurement-error and Ising process models. We also discussed initialization of the MAP iteration and applied the proposed detector to simulated eddy-current and experimental ultrasonic C-scan data. Further research will include

- developing a false-discovery-rate (FDR) based method (see e.g. [7]) that utilizes a realistic ultrasonic noise and signal models and
- applying the HMRF framework to other NDE problems with focus on data fusion.

ACKNOWLEDGMENT

This work was supported by the NSF Industry-University Cooperative Research Program, Center for Nondestructive Evaluation (CNDE), Iowa State University.

REFERENCES

1. Cressie, N.A.C., *Statistics for Spatial Data*, revised ed., New York: Wiley, 1993.
2. Besag, J., *J. R. Stat. Soc., Ser. B,* **48**, 259–302 (1986).
3. Vengrinovich V.L. *et al.*, *J. Phys. D: Appl. Phys.,* **32**, 2505–2514 (1999).
4. Fukunaga, K., *Introduction to Statistical Pattern Recognition,* 2nd ed., San Diego, CA: Academic Press, 1990.
5. Hand, D.J., *Discrimination and Classification,* New York: Wiley, 1981.
6. Dogandžić, A and Eua-anant, N., *Review of Progress in QNDE,* Vol. 23, eds. D.O. Thompson and D.E. Chimenti, AIP, Melville New York, 2003, pp. 628–635.
7. Benjamini Y. and Hochberg Y., *J. R. Stat. Soc., Ser. B,* **57**, 289–300 (1995).